Nonmodal Gating of Cardiac Calcium Channels as Revealed by Dihydropyridines

ANTONIO E. LACERDA and ARTHUR M. BROWN

From the Department of Molecular Physiology and Biophysics, Baylor College of Medicine, Houston, Texas 77030

ABSTRACT The hypothesis that dihydropyridine (DHP)-sensitive calcium channels have three distinct modes of gating has been examined. The major prediction is that the relative frequencies among modes depend on DHP concentration while the kinetics within a mode do not. We tested this by studying whole-cell and single-channel calcium currents in neonatal rat and adult guinea pig cardiac myocytes in different concentrations of several DHPs. In the absence of DHPs calcium currents declined with time but the kinetics, which are the focus of this study, were unchanged. Open-time frequency distributions had insignificant numbers of prolonged openings and were well fit by single τ's. Agonist DHP stereoisomers produced concentration-dependent changes in whole-cell tail current τ's. The frequency distribution of single calcium channel current open times became biexponential and the τ's were concentration dependent. The average number of openings per trace of channels with customary open times increased with increases in DHP concentration. Latencies to first opening for the customary openings and for prolonged openings were shorter in the presence of DHPs. A second larger conductance is another important feature of DHP-bound single calcium channels. Thus DHPs not only caused prolonged openings; they produced numerous changes in the kinetics of customary openings and increased channel conductance. It follows that these effects of DHPs do not support the hypothesis of modal gating of calcium channels. The mode model is not the only model excluded by the results; models in which DHPs are allowed to act only or mainly on open states are excluded, as are models in which the effects are restricted to inactivated states. We suggest a different type of model in which cooperative binding of DHPs at two sites produces the essential changes in kinetics and conductance.

INTRODUCTION

A widely proposed hypothesis for voltage gating of dihydropyridine (DHP)-sensitive calcium channels is the mode hypothesis. This states that gating has three modes, two of which are stabilized by DHPs (Hess et al., 1984, 1985*a*, *b*; Reuter et al., 1985, 1986; Tsien et al., 1985; Fox et al., 1986; Kokubun et al., 1986). It is suggested that switching among modes is physiological, perhaps endogenously regulated (Nowycky et al., 1985*a*; Fox et al., 1986). Mode 1 is the usual gating mode, mode 2 has greatly

Address reprint requests to Dr. Arthur M. Brown, Department of Molecular Physiology and Biophysics, Baylor College of Medicine, One Baylor Plaza, Houston, TX 77030.

J. GEN. PHYSIOL. © The Rockefeller University Press · 0022-1295/89/06/1243/31 $2.00
Volume 93 June 1989 1243–1273

prolonged open times and mode 0 is an inactivated state. The modes are reversibly interconnected and to be identifiable, the transitions among modes must be much slower than the transitions within modes. The main evidence is that the DHP agonist Bay K 8644 produces numerous prolonged openings that are far less frequent in the absence of drugs i.e., Bay K 8644 stabilizes mode 2. Nimodipine, a DHP antagonist, is thought to stabilize mode 0, and mode 1 is not thought to bind DHPs.

Other models have been proposed to account for the single-channel effects of DHPs and they share the feature that DHPs are thought to alter a particular gating sequence rather than the frequency with which putative modes are occupied. In one, Bay K 8644 reduces the transition rate constant from open to closed by a factor of 10 (Sanguinetti et al., 1986). In another, DHPs combine only with the open channel to produce their effects (Bechem and Schramm, 1987). In a third, DHPs have both high and low affinity sites and DHP-bound channels show complex changes in kinetics, including increased frequencies of channel opening, prolonged channel openings in the case of agonists, or increased nulls and decreased opening probability in the case of antagonists (Brown et al., 1984*a*, 1986). Finally, there are some models in which DHP inhibition alone was analyzed (Bean, 1984; Gurney et al., 1985; Cohen and McCarthy, 1987) and in which the modulated receptor hypothesis (Hille, 1977; Hondeghem and Katzung, 1977) was applied. Because a consensus has not been reached, we reexamined the effects of DHP stereoisomers on single and whole-cell calcium channel currents. Particular attention was paid to the mode model because it is the most widely quoted and because it has the fewest constraints. In addition to causing prolonged openings, DHPs produced pronounced changes in the kinetics of the single-channel and whole-cell currents customarily observed in the absence of DHPs. An additional finding of importance is that DHP agonists increase calcium channel conductance. Our results do not support the mode model as an explanation for the effects of DHPs and by implication as an explanation of calcium channel gating. The models with binding restricted to an open state or an inactivated state are also rejected. Instead we propose an extended version of our earlier model (Brown et al., 1986) in which two DHP sites are cooperatively linked to produce their effects on single-channel and whole-cell currents.

MATERIALS AND METHODS

Preparation of Cardiac Cells

Neonatal rat heart ventricular myocytes were prepared by a modification of the method of Mark and Strasser (1966). Briefly, ventricular cells were obtained for primary culture by trypsin (Sigma Chemical Co., St. Louis, MO) digestion of 1–3-d-old neonatal ventricular tissue cut into 1–2-mm cubes. Cells were cultured on 9-mm square poly-D-lysine (Sigma Chemical Co.) coated glass coverslips on the bottom of 35 × 10 mm Falcon plastic tissue culture dishes (Beckton, Dickinson and Co., Oxnard, CA) in a 1:1 mixture of Dulbecco's modified Eagle's medium and Ham's F12 medium (Gibco Laboratories, Grand Island, NY) with HEPES buffer at 37°C in a water-saturated air atmosphere. Cells were used 1–2 d after plating. Adult guinea pig cardiac myocytes were prepared as described by Powell et al. (1980).

Experimental Recording

Whole-cell, cell-attached and outside-out patch-clamp experiments (Hamill et al., 1981) were performed using a List EPC-7 amplifier (List Electronics, Darmstadt, FRG) and patch-clamp electrodes fabricated from 7052 glass tubing (Garner Glass Co., Claremont, CA). Electrodes of <2 MΩ resistance were used for whole-cell recordings. Series resistance error was reduced by adjusting the series resistance compensation circuit of the EPC-7 to just below the point of ringing. For some experiments pipettes were coated with Sylgard (Dow Corning Corp., Midland, MI).

For whole-cell and most single-channel experiments the bath was superfused continuously with control and drug containing solutions at rates of 1–2 ml/min. The superfusion apparatus was constructed of teflon tubing and valves with glass solution reservoirs. Clear RTV (room temperature vulcanizing) #9 silicone adhesive sealant (Master Chemical Corp., Memphis, TN) was diluted with benzene and manually applied as a coating for the aluminum chamber used in these experiments, and in undiluted form to attach a circular coverglass to make the bottom of the chamber. Chamber volume was varied between 0.2 and 0.5 ml which provided exchange rates of 2–10 vol/min. Inlet and outlet ports were arranged to provide solution flow directly across the cells. The reference electrode was a chlorided Ag wire connected to the bath by a 1 M KCl/agar bridge. This electrode was placed downstream from the cells next to the outlet port. The experimental chamber and superfusion apparatus were washed with 70% ethanol and distilled water between experiments, although this did not always prevent contamination by DHPs of control and low dose data.

Data Acquisition and Analysis

All data were filtered by an 8-pole Bessel filter to 0.3 of the sampling frequency (−3 dB point) and digitized into 2,048-point records at rates up to 100 kHz by an LSI 11/73 minicomputer. The computer simultaneously sampled current and provided command voltages to the patch clamp through 12-bit analog-to-digital and digital-to-analog converters. Whole-cell data were corrected by an on-line summing procedure that added a variable, predetermined number (usually 2) of scaled and inverted pulses to a single depolarizing pulse and stored the sum on a hard disk. The single-channel data were corrected by averaging nulls and subtracting the average from each record. When further correction was necessary a spline curve was fitted to any remaining capacitive transient of the corrected records at the end of the voltage step and subtracted from the transient at the beginning of the step. The corrected data were then analyzed with an interactive level detection program that could be run automatically after threshold parameters were set. Openings were detected by setting thresholds at half the open-channel amplitude (Colquhoun and Sigworth, 1983) of the predominant type of opening. To enhance detection records were reanalyzed with different thresholds as required. The output of the program displayed raw, digitally filtered, and idealized events simultaneously on an oscilloscope. Parameter estimates, with the exception of unitary current amplitudes and the number of openings in a burst, were obtained from idealized channel data by the maximum-likelihood method as described in Colquhoun and Sigworth (1983), including correction for truncation of probability density functions by minimum and maximum resolvable intervals. Nonlinear least-squares and maximum-likelihood criteria were used to estimate parameters for the sum of Gaussian distributions. All amplitude histograms shown were constructed from idealized events. We used idealized events to eliminate the weighing of event amplitudes by their open times when histograms are constructed from all points in the ensemble of records without idealization. This is a concern in constructing out amplitude histograms since mean open times of fast and slow openings differ by a factor of 10–20 in (−)

Bay K 8644–treated patches. A comparison was made between amplitude histograms at 0 mV of idealized and raw data in control and (−) Bay K 8644 at 100 nM. The idealized data gave mean values of 1.59 (drug) and 1.03 (control) pA for the largest amplitude peak (Fig. 10, below). The raw data gave values of 1.62 (drug) and 1.45 (control) pA. The maximum-likelihood estimate of the number of openings in a burst was obtained from the sum of geometric distributions. Macroscopic tail currents were fit by nonlinear least squares. All of our fitting algorithms used the Marquardt-Levenberg optimization procedure implemented as described in Bevington (1969).

For burst detection, we assigned values for the maximum closed time in a burst according to:

$$1 - e^{-t_c/\tau_s} = e^{-t_c/\tau_f} \quad (1)$$

where t_c is the critical gap (closed time) duration that signifies termination of a burst, τ_f is the time constant of the gaps within a burst, and τ_s is the time constant of the gaps between bursts (Colquohoun and Hawkes, 1982; Colquhoun and Sakmann, 1985). We used values of τ_f and τ_s obtained from maximum-likelihood parameter estimates for closed-time distributions, and solved for t_c, the critical gap length. The probabilities of a closed interval arising from either the fast or slow component of the closed-time distribution are equal at t_c. This method of choosing a critical gap length produces proportionate errors in assigning closed times to closed intervals within bursts (τ_f) and to closed intervals between bursts (τ_s).

Solutions

For whole-cell experiments neonatal rat ventricular myocytes attached to glass coverslips were maintained in the experimental chamber during seal formation in a nominally Ca-free Tyrode's solution of composition (in millimolar): 135 NaCl, 5.4 KCl, 2 $MgCl_2$, 10 HEPES, 10 glucose, pH 7.4, adjusted with *N*-methyl-D-glucamine (NMG). For recording whole-cell Ca^{2+} channel currents, the external solution composition was (in millimolar): 5 $CaCl_2$, 105 NMG, 115 aspartic acid, 30 TEA-Cl, 5 4-AP, 10 HEPES, pH 7.4, adjusted with NMG. Basic internal solution composition was (in millimolar): 126 NMG, 98 aspartic acid, 11 EGTA, 0.1 $CaCl_2$, 2 $MgCl_2$, 20 CsF or NMG-F, 10 HEPES, pH 7.45, adjusted with NMG. The following additions were made to 10 ml of chilled basic internal solution (in millimolar): 0.5 cAMP, 2 Na_2ATP, 0.5 Na_2GTP, 0.1 leupeptin, 1 theophylline, and (in milligrams): 0.1 protein kinase A (regulatory and inhibitory subunit complex, Sigma Chemical Co.), 0.1 γ-S-ATP, 0.1 γ-S-GTP. This solution was thoroughly mixed in a cold room for 5 min and then kept in a syringe on ice for the duration of the experiment. At room temperature the pH of the resulting solution was ~7.2.

Solutions used for cell-attached single-channel experiments consisted of an external depolarizing solution for most neonatal rat and adult guinea pig ventricular myocyte data. Some data were obtained with a normal Tyrode's bath solution (described above with the addition of 2 mM $CaCl_2$). The depolarizing solution had the following composition (in millimolar): 140 K-aspartate, 10 EGTA, 10 HEPES at pH 7.4 (adjusted with NMG). The pipette solution for cell-attached patches was (in millimolar): 100–110 $BaCl_2$, 10 HEPES, pH 7.4, adjusted with NMG. For some experiments the temperature of the bath was increased to 32–37°C with battery-powered Peltier effect devices (Melcor, Trenton, NJ) arranged inside a negative feedback control loop to maintain the bath at a desired temperature.

Source of Stereoisomers

We used stereoisomers (>95% purity) rather than racemic mixtures because of the functional differences between stereoisomers. Dr. Scriabine of Miles Laboratories, New Haven, CT gen-

erously provided the Bay K 8644 stereoisomers and racemic nitrendipine (NTD). Stereoisomers of 202-791 were gifts from Dr. R. Hof of Sandoz Ltd., Basel, Switzerland.

RESULTS

Whole-Cell Currents

Current stability. We used large pipettes to observe fast components of calcium currents in spherical cultured neonatal rat myocytes with cell diameters in the 10–15 μm range. Without any additions to the pipette solution, rapid and irreversible rundown of the calcium currents occurred (Cota, 1986; Matteson and Armstrong, 1986). With the additions described in Methods the rate of rundown slowed and recording of tail τ's through three or more solution changes of a cumulative dose-response relation (increments in log units of concentration) and a final washout period was possible. Related internal solutions were used by Cota (1986), in rat pituitary pars intermedia cells, and Chad and Eckert (1986), in snail neurons, to reduce rundown. In experiments with smaller pipettes, more stable calcium currents can be recorded from neonatal cells for >40 min. Rundown appeared to occur exclusively as a simple scaling of the current amplitudes; no detectable changes in time course occurred. The process was tracked at the start of the experiments and by assuming it to be linear could be corrected for when this made presentation clearer (inset of Fig. 1).

Peak currents. Peak current records from a cell bathed in 5 mM Ca^{2+} solution in control and in 1 μM (−) Bay K 8644 are shown superimposed in Fig. 1. For the currents in Fig. 1 (−) Bay K 8644 reduces the time to peak and increases the rate of current decay during the step (Hess et al., 1984). Due to rundown of the calcium channels, current in (−) Bay K 8644 appears to crossover the control current to a lower value at the end of the pulse. In the absence of rundown the currents would not have crossed over during the 8 ms step (inset, Fig. 1). The inset of Fig. 1 shows overlaid current records from control, 1 μM DHP, and washout data. A current record obtained 20 min after control after washout of (−) Bay K 8644 was scaled by a factor of four to overlay the initial control current record. This was approximately the value estimated by assuming linear rundown. A factor of four was also used to scale the current in 1 μM (−) Bay K 8644. After applying this correction for rundown, peak current in 1 μM (−) Bay K 8644 was increased 3.8-fold over control, a factor within the range described by others (Brown et al., 1984*a*; Hess et al., 1984; Sanguinetti et al., 1986).

Fenwick et al. (1982) and Cota (1986) also attribute the effects of rundown to changes in the availability (number) of functional calcium channels without alteration of channel kinetics. Cota (1986) found the addition of MgATP and GTP to his internal solution necessary to prevent a slow hyperpolarizing shift of whole-cell calcium current activation in GH_3 cells; these compounds were always present in our internal solution and our whole-cell current kinetics appeared stable (compare control and washout records in inset of Fig. 1). The most significant correlation we have observed between current magnitude and channel kinetics is due to series resistance errors.

Dependence of tail current τ's on DHP concentration. A model in which DHPs stabilize a mode with a prolonged open state might be expected to produce relaxations with stereotyped exponential time constants for different concentrations of DHPs. Only the amplitude coefficients would change. Such stereotyped behavior did not occur. Figs. 2 and 3 show that the τ's of the slow tails were concentration dependent. In Fig. 2 tail currents from neonatal cells were fitted by nonlinear least squares with the sum of two exponentials in control and in the presence of (−) Bay K 8644. Fig. 2 *A* shows a biexponential fit to a tail current measured at −50 mV in the absence of (−) Bay K 8644. The fit of the sum of two exponentials was better

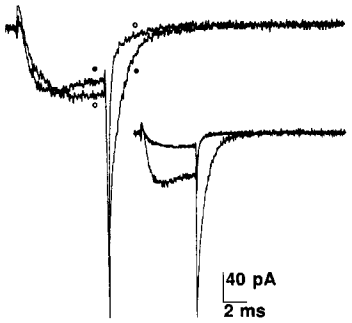

FIGURE 1. Whole-cell current response to a voltage step. Current records from one neonatal ventricular myocyte in 5 mM $CaCl_2$ are shown in control (*open circles*) and in 1 μM (−) Bay K 8644 (*filled circles*) with tail currents obtained at −90 mV. The data are shown digitally filtered with a 4-pole, zero-phase filter to 3 kHz bandwidth. The pulse protocol used was to hold at −50 mV, step to 20 mV for 8 ms, and return initially to −90 mV at a rate of 0.17 Hz. The return potential was incremented in 10-mV steps to −20 mV and the series repeated at 30-s intervals. Currents were corrected by a P/2 procedure during the interval between depolarizing pulses. For the P/2 correction the cell holding potential was changed to −70 mV from −50 mV 200 ms before each of two inverted pulses of half amplitude were applied at 0.5 Hz. At the end of each inverted pulse the holding potential was returned to −50 mV. The inverted pulses were summed on line and the sum was stored on a hard disk. Data were analog-filtered at 30 kHz (−3 dB point) by an 8-pole Bessel filter before conversion to digital form at 100 kHz. In the presence of (−) Bay K 8644, current during the step shows a reduced time to peak and an increased rate of current decay. The inset shows three current records overlaid. In addition to the control and drug traces shown in the main figure, a record from late in the washout period is shown scaled by a factor of 4 to overlay the control record from the main figure. The same scaling factor of 4 was used in the inset to correct the current trace in 1 μM (−) Bay K 8644 for the effect of rundown. Calibration bars refer to the main figure.

than the fit of a single exponential at the 95% or greater confidence level using *F* test criteria. Panels *B* and *C* of Fig. 2 show that the effect of (−) Bay K 8644 on tail currents is not simply to scale the amplitude of statistically indistinguishable τ's. The upper record in both Fig. 2, *B* and *C* show the best nonlinear least-squares fit to tail currents obtained at −20 mV in the presence of 0.1 (*B*) and 1 (*C*) μM (−) Bay K 8644 with both fast and slow component τ's and amplitudes free to vary. The lower record in Fig. 2 *B* shows the same data as in the upper record but fit with the slow τ obtained at 1 μM (−) Bay K 8644 and the fast τ from the data at 0.1 μM drug. Similarly, the lower record in Fig. 2 *C* is the same as the upper but fit with the fast τ

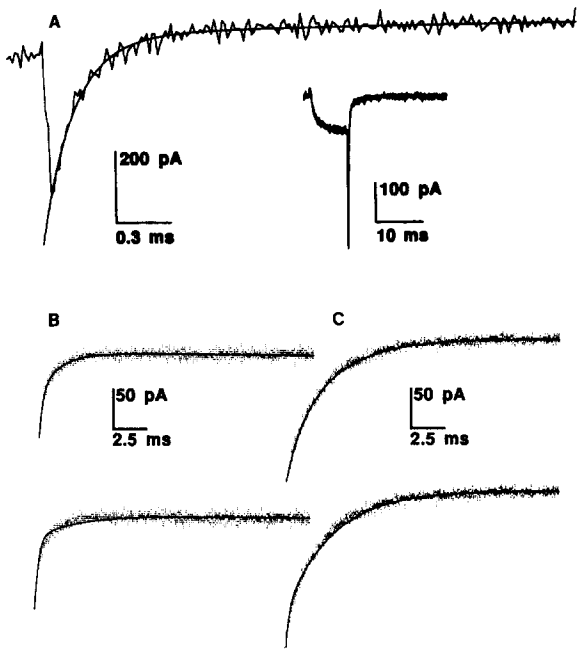

FIGURE 2. Fit to tail currents from a neonatal ventricular myocyte in 5 mM $CaCl_2$ bath solution. In *A* a tail current at −50 mV from the neonatal ventricular myocyte shown in Fig. 1 is fitted by nonlinear least squares with two exponentials having fast and slow τ's of 0.17 and 2.03 ms, and amplitudes of −603 and −43 pA, respectively, in the absence of (−) Bay K 8644. Data were analog-filtered at 30 kHz (−3 dB point) by an 8-pole Bessel filter before conversion to digital form at 100 kHz. The inset shows the entire current record. The current in the inset is smoothed to emphasize the slow component of the tail. The pulse protocol is the same as described in Fig. 1. Series resistance compensation was adjusted after this pulse series. In *B* tail currents in 0.1 (upper and lower records) and in *C* in 1 μM (upper and lower records) (−) Bay K 8644 at −20 mV, obtained from the same cell with series resistance compensated for, are shown. The records shown are the average of two tail currents in both *B* and *C*. The upper record in both *B* and *C* is fit by nonlinear least-squares criteria with the sum of two exponentials with amplitude and τ of each component free to vary. For comparison the lower record in *B* is the same data but fit with the slow τ from the fit to the upper record in *C* at 1 μM (−) Bay K 8644 and the fast τ from the fit at 0.1 μM drug. Conversely, the fast τ from the fit at 0.1 μM drug and the slow τ from the fit at 1.0 μM drug are used to fit the 1 μM data in the lower record in *C*. Only the amplitudes of the fast and slow components were allowed to vary in the fits to the data in the lower records of *B* and *C*. Visually better fits are obtained when τ's are allowed to vary, indicating that the concentration dependence of tail current τ's is not an artifact of the fitting procedure. Fits with τ's free to vary were significantly better by the *F* test criterion at the 99% confidence level. Values in the upper record of *B* for the fast τ and the amplitude of the fast component were 247 μs and −83 pA, respectively, and those of the slow τ and the amplitude of the slow component were 1,570 μs and −54 pA, respectively. Values in the upper record of *C* for the fast τ and the amplitude of the fast component was 982 μs and −60 pA, respectively, and those of the slow τ and the amplitude of the slow component were 3,607 μs and −174 pA, respectively. Values in the lower record of *B* for the fast and slow τ amplitudes were −135 and −31 pA, respectively, and in *C* they were −84 and −193 pA, respectively. Data in *B* and *C* were digitally filtered at 5 kHz with a 4-pole zero-phase filter.

from the 0.1 μM data and the slow τ from the 1 μM data. In the lower records of Fig. 2, *B* and *C* only the amplitudes of both components were free to vary. The fits to the upper records in Fig. 2, *B* and *C* with amplitudes and τ's free to vary are significantly better than the fits in the lower records with constrained τ's at greater than the 95% confidence level by the *F* test criterion. This suggests that (−) Bay K

8644 can alter deactivation τ's in a concentration-dependent manner and that we can distinguish this from a change in the weighting of fast and slow components with fixed τ's.

The relationship between the slow tail current τ's and DHP concentrations up to 1 μM is shown in Fig. 3. Using nonlinear least squares the data in Fig. 3, *A* and *B* were fit to a single-site binding model with ED_{50}'s of 21 and 39 nM, respectively. These values are close to other estimates of ED_{50} for Bay K 8644 agonist effects: racemic Bay K 8644, 30 nM (Brown et al., 1984*a*, 1986); (−) Bay K 8644, 5 nM

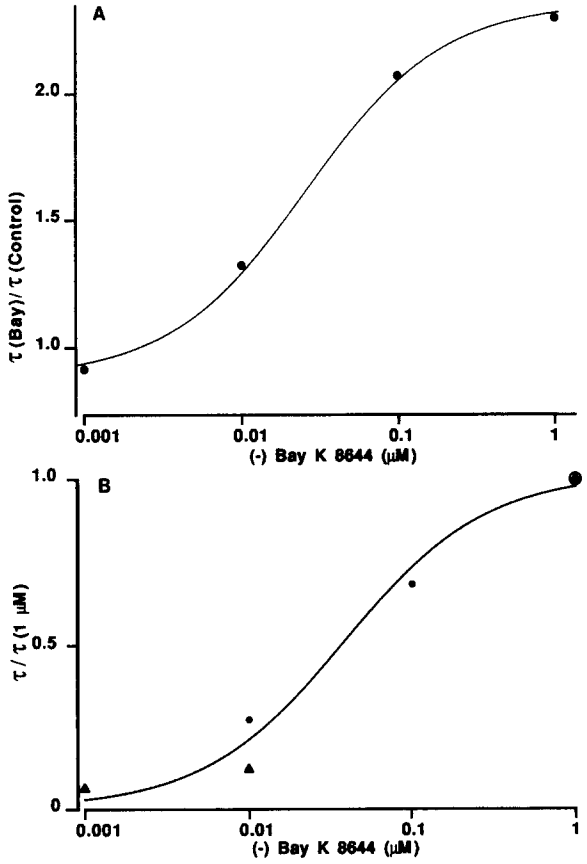

FIGURE 3. Concentration-response relationship for the whole-cell slow tail current τ in 5 mM $CaCl_2$. Concentration dependence of the slow tail current τ from another neonatal ventricular myocyte is shown in *A*. An ED_{50} of 21 nM was obtained from a nonlinear least-squares fit of a single-site binding model to the data. Each point is the mean of the ratio of slow τ tail currents in (−) Bay K 8644 to control measured at −50, −40, and −30 mV in each concentration. *B* shows the concentration dependence of the slow tail current τ at −50 mV from the cell shown in Figs. 1 and 2 (*circles*) and a third neonatal ventricular myocyte (*triangles*) each normalized by the value of their respective slow tail current τ at −50 mV in 1 μM (−) Bay K 8644. A nonlinear least-squares fit of the data produced an ED_{50} of 39 nM. Each symbol corresponds to one measurement.

(Bechem and Schramm, 1987); and from binding experiments; 2.4 nM (Janis et al., 1984), 35 nM (Bellemann, 1984), and 25 nM (Bellemann and Franckowiak, 1985). With peak current measurements Brown et al. (1986) observed at higher DHP concentrations a low affinity site with an ED_{50} of 0.9 μM. Although we conclude that a multiple binding site model best describes our data (see Discussion) we did not fit the data to a multiple binding site model for several reasons. Our range of concentrations did not span the low affinity binding region and the number of different concentrations applied precludes detecting ED_{50}'s that are not very well separated

within the range of concentrations used. Since a good fit was obtained with one binding site, the addition of a second site would not produce a significantly better fit.

The fast tail τ's were also prolonged at higher concentrations. However, their variability precluded a reasonable fit of an ED_{50} to the concentration-τ data. Fig. 4 shows the voltage dependence of the fast tail current τ in control and at 1 μM (−) Bay K 8644. (−) Bay K 8644 appears to simply scale the τ-voltage relation and has little effect on the exponential shape of the curve. The effects of (−) Bay K 8644 were slowly reversible and tail τ's decreased during the washout period to values differing from control by < 40% for this cell. Similar recovery was seen in two additional cells in which washout was performed. We observed a concentration dependence of the fast τ in two cells and examined the voltage dependence of the fast τ in

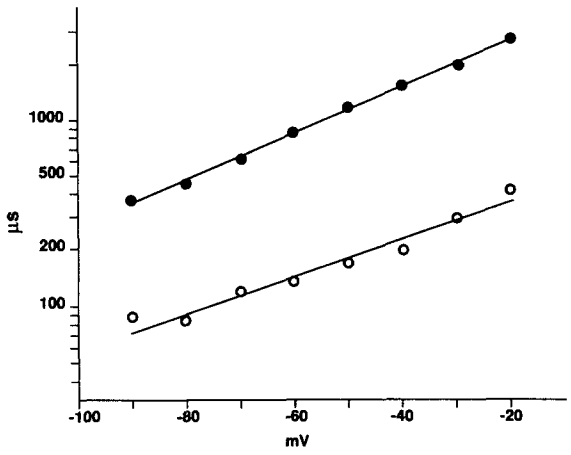

FIGURE 4. Fast tail τ's from whole-cell clamp data in 5 mM external $CaCl_2$. Tail τ's from a neonatal ventricular myocyte are shown plotted semilogarithmically as functions of voltage in control (*open circles*) and at 1 μM (*filled circles*) (−) Bay K 8644. The data are fit with linear least-squares lines with slopes of 100 μs/decade mV (r = 0.98) and 79 μs/decade mV (r = 0.99) for control and DHP, respectively. (−) Bay K 8644 produces minor changes in the voltage dependence of the fast τ's from control to 1 μM DHP concentration. The fast tail τ's in this voltage range maintain an exponential dependence on voltage in the presence of DHP. We found a slowing of the fast τ in the presence of 1 μM (−) Bay K 8644 in two neonatal ventricular myocytes.

one. Bechem et al. (1987) have also described a lack of effect of Bay K 8644 on the τ-voltage relation and a scaling of the concentration-τ relation in guinea pig atrial myocytes. Fenwick et al. (1982) and Brown et al. (1984*b*) in chromaffin cells and snail neurons, respectively, reported similar τ values and a similar voltage dependence for the fast component of calcium current deactivation.

Low threshold Ca^{2+} channels (Carbone and Lux, 1984; Bean, 1985; Nilius et al., 1985) are present in neonatal myocytes (Lacerda and Brown, 1986). As in GH_3 cells, low threshold channels have slow deactivation tail τ's (Cota, 1986; Matteson and Armstrong, 1986). Our pulse protocols were designed to eliminate tail current components due to low threshold channels by holding cells at −50 or −40 mV, potentials at which these channels are completely inactivated at the whole-cell level (Carbone and Lux, 1984; Bean, 1985; Matteson and Armstrong, 1986). Furthermore, low threshold channels are not sensitive to DHPs (Bean, 1985; Nilius et al., 1985)

and tail currents corresponding to low threshold channels are not seen with pulses of long duration. We have fitted in control conditions tail currents at depolarized holding potentials from six cells with the sum of two exponentials in 5–40 mM Ba^{2+} and Ca^{2+} solutions after both long (> 100 ms) and short pulses without observing a component attributable to low threshold Ca^{2+} channels.

Hume and Uehara (1986) described slow tail currents in frog atrial cells, which they attributed to the activity of an electrogenic Na^+/Ca^{2+} exchanger. Inward "creep current" in this mechanism is carried by an influx of Na^+ ions in exchange for internal Ca^{2+} ions. This current is unlikely to be present in our experiments. The internal solution we used had free Ca^{2+} buffered to $<10^{-9}$ M while the external solution contained only Ca^{2+} and Cl^- inorganic ions and was superfused continuously. The kinetics of creep currents are 1–2 orders of magnitude slower than the τ's we observe and are prominent only in Na^+-loaded cells. Another potential tail current component might arise from monovalent cation fluxes through the nonspecific cation channel activated by internal Ca^{2+} transients. If this occurred, the only major inorganic monovalent cations are internal Na^+ at 4 mM and, in preliminary experiments, internal Cs^+ at 20 mM, both of which would produce outward "creep current" tails since they are likely to be much more permeable than the major cation, NMG^+. In fact, any alteration of tail currents indirectly through a Ca^{2+}-linked process is unlikely because currents such as those shown in Fig. 1 produced similar Ca^{2+} transients during the depolarizing steps in control and 1 μM (−) Bay K 8644, but had very different tail currents. In two experiments with Ba^{2+} solutions we observed two component tail currents similar in kinetics to those shown here in Ca^{2+}-containing solutions under control conditions.

Single Ca^{2+} Channel Currents

A direct comparison of whole-cell with single-channel data is not possible due to the large voltage shift in Ca^{2+} channel gating induced by ~100 mM divalent ion concentrations. We observe a shift of 30–40 mV in gating of Ca^{2+} channels in whole-cell data over a range of 2–100 mM Ca^{2+}. A discussion of divalent ion induced shifts in gating of Ca^{2+} channels can be found in Wilson et al. (1983), and of cardiac calcium channels in Kass and Krafte (1987). Our main purpose is to study the effects of DHPs so direct comparisons are not essential.

Open-time data. The frequency histogram of open times for single calcium channels in cell-attached patches can be described by a single exponential distribution in the absence of DHP agonists (Brown et al., 1982; Fenwick et al., 1982; Reuter et al., 1982; Cavalié et al., 1983, 1986) but a sum of two exponential distributions is required in their presence (Hess et al., 1984; Kokubun and Reuter, 1984; Ochi et al., 1984). Most of our cell-attached patches from primary cultures of neonatal rat cardiac myocytes have a low frequency of Ca^{2+} channel opening events at room temperature. Thus the absence of a slow τ due to prolonged openings in the open-time histogram from control data may be the result of a small sample size. Cavalié et al. (1986), however, analyzed 71 cell-attached patches on adult guinea pig ventricular myocytes at temperatures of 32–37°C where the frequency of events is much greater. They concluded that open-time histogram data were best described by a single exponential function.

To increase the frequency of openings we raised the temperature of the bath from 20°C to 32–37°C. The channel opening activity of control cell-attached patches was increased severalfold. Fig. 5 *A* shows data from a cell-attached patch on a neonatal rat myocyte at 32°C. This patch had 887 openings in 100 pulses to 10 mV

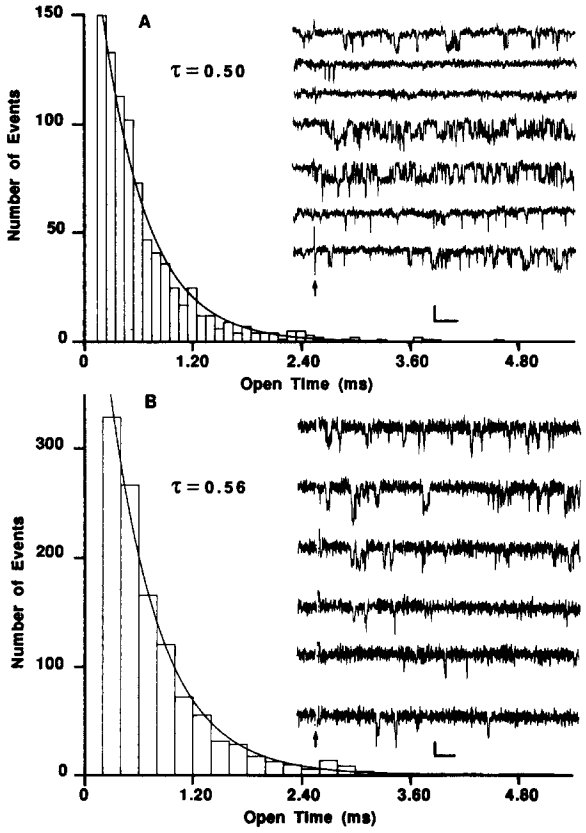

FIGURE 5. Control open-time distributions. Histogram of the open-time distribution from a cell-attached patch on a neonatal ventricular myocyte at 32°C with 140 mM K-aspartate depolarizing solution in the bath (*A*) and from an adult guinea pig ventricular myocyte with Tyrode's solution in the bath at 34°C (*B*). Pipettes in both *A* and *B* were filled with 100 mM $BaCl_2$ solution. Arrow below current records signifies onset of voltage pulse. Open-time distribution parameters were obtained with the maximum-likelihood method and simultaneous openings were excluded from the analysis. The open-time τ for the neonatal ventricular myocyte in *A* was 0.50 ms at a step potential of 10 mV, holding potential of −40 mV, pulse frequency of 1 Hz, and an analog filter frequency of 3 kHz (−3 dB). The data were not subsequently filtered. The adult guinea pig ventricular myocyte in *B* had an open-time τ of 0.56 ms. The patch was held at rest, a 70-mV depolarizing step was applied at a frequency of 0.2 Hz, and the final filter frequency was 1 kHz (−3 dB). In *A* one opening at 13 ms is not shown (total number of events, 887) and in *B* two openings at 7.2 and one at 8 ms are not shown (total number of events, 1,023). Six overlapping openings were detected giving an observed probability of 6:1,119 or 5.4×10^{-3}. The expected probability of overlapping openings is 0.6×10^{-3} from the binomial distribution for two independent, identical channels each with a P_o of 0.024 (calculated as in the text). Equally infrequent occurrences of long openings under control conditions were observed in eight neonatal ventricular myocytes at room temperature. Calibration: vertical, 1 pA; horizontal, 10 ms.

of 130 ms duration. Only two openings were longer than 5 ms (maximum 13 ms). Two channels were present in the patch based on the maximum number of overlapping events observed and binomial expectation. Five overlapping openings were detected for an observed probability of 5.6×10^{-3}. The expected probability under

binomial assumptions for overlapping openings at P_o 0.035 was 1.2×10^{-3}. P_o was calculated as the ratio of ensemble mean current to the mean unitary current amplitude obtained from nonlinear least-squares fits of Gaussian distributions to histograms of unitary current amplitudes. These data indicate that long-lived openings are rare, no more than 0.23% of openings in this cell. In another cell-attached patch, in this case from an adult guinea pig ventricular myocyte, two channels were present in the patch based on the maximum number of overlapping events and binomial expectation. There were 1,119 openings at 32°C with six overlapping events and only three openings longer than 6 ms (maximum 8 ms) (Fig. 5 *B*). These data are typical for 10 control cells when the recording setup had not been used in DHP experiments for several weeks, as was the case for these cells. Cavalié et al. (1986) have also described the paucity of mode 2 openings in their data, only 2 patches of 71 had long openings and in both instances these openings were <1% of all openings. Our results, those of Cavalié et al. (1986), and those of Hoshi and Smith (1987) at potentials negative to 10 mV differ from the results of Nowycky et al. (1985*a*) and Fox et al. (1986) who have reported mode 2 openings occurring in >10% of control records. We did not observe a significant number of prolonged openings in control data from eight other cells at room temperature. Thus in our hands a major implication of the mode model, that mode occupancy is endogenously regulated, is difficult to evaluate because of the rarity with which the pertinent events—the mode 2 openings—occur.

Clustering of prolonged openings is characteristic of mode gating (Hess et al., 1984; Nowycky et al., 1985*a*). Obvious clustering of prolonged openings in either our control or our DHP data analogous to that already described did not occur. In bovine chromaffin cells clustering was not characteristic of depolarization-induced prolonged openings, and both long and short openings occurred in the same trace in the presence of Bay K 8644 (Hoshi and Smith, 1987). Most of our patches have few openings in control conditions and contain more than one Ca^{2+} channel. In the presence of DHP clustering of openings may be obscured in multichannel patches. We note that records with relatively high P_o can occur in the absence of prolonged openings and that these records may appear clustered. The fourth and fifth current records in Fig. 5 *A* are two of three consecutive traces each separated by 1 s. These three records each had more than 60 openings with a mean NP_o of 0.53 ± 0.05, while the next largest NP_o is 0.17. Nonetheless, only one opening longer than 5 ms was observed in this patch. Hence clustering may not uniquely identify mode gating of prolonged openings. These data were obtained at 3 kHz (−3 dB point) bandwidth. The binomial analysis of clustering for the single-channel case as described in Nowycky et al. (1985*a*) overestimates the nonrandomness of clustering of prolonged openings since the null hypothesis tested is based on prolonged openings being independent of each other. Successive open times in the nicotinic ACh receptor are correlated, and simpler Markovian models rather than modal models accounted for the results (Jackson et al., 1983; Colquhoun and Hawkes, 1987). For a channel in so-called mode 2 with bursting kinetics, it may be more appropriate to analyze the probability of consecutive bursts being of the same type rather than consecutive openings.

Open-time histograms show a concentration-dependent increase in open time

with (−) Bay K 8644. Fig. 6 shows the slow τ of the open-time histogram from a cell-attached patch on a neonatal rat ventricular myocyte fit with a one-site binding model. The data were obtained at a step potential of 20 mV, holding potential of −40 mV, and were fit by nonlinear least squares with an ED_{50} of 49 nM. Independently of the estimated τ values, the length of the longest opening observed increases with concentration by a factor of ~10 between 10 and 1,000 nM, while the number of observations at the high and low concentrations remains relatively constant. An estimate of two channels present in this patch was based on the maximum number of overlapping events observed. A binomial probability of 0.033 for the

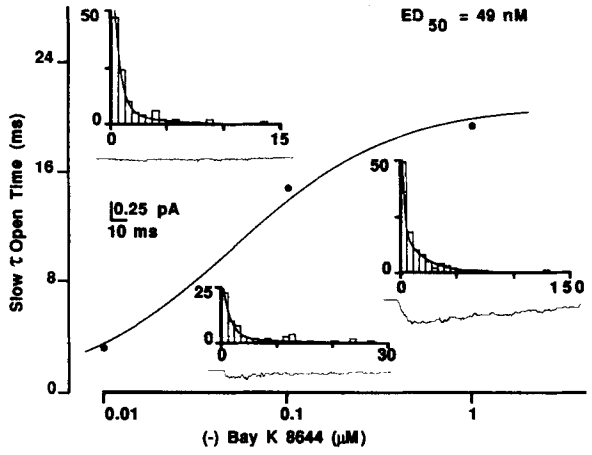

FIGURE 6. Concentration dependence of slow open-time τ. Maximum-likelihood estimates of the slow open-time τ from a neonatal ventricular myocyte are shown as a function of (−) Bay K 8644 concentration. Cell-attached recording with 100 mM $BaCl_2$ in the pipette and 140 K-aspartate depolarizing solution in the bath. The cell was held at −40 mV and stepped alternately to 20 and 0 mV at 1 Hz. The data shown were obtained at 20 mV and are fit with a single binding site model with an ED_{50} of 49 nM. Open-time histograms and sums of idealized channel currents correspond to increasing concentrations of (−) Bay K 8644 from left to right. The maximum-likelihood parameter estimates from open-time data are shown superimposed on histograms of the open-time distributions. Note the change in the maximal time value in each histogram. The pulse duration is the same in each sum of idealized traces: 130 ms. Maximum-likelihood estimates of the fast τ were 0.54, 1.61, and 1.59 ms at 10, 100, and 1,000 nM (−) Bay K 8644, respectively. Data were filtered at 1 kHz by a 4-pole zero-phase digital filter. Data were analog filtered by an 8-pole Bessel filter at 3 kHz (−3 dB) when digitized. We observed an increase of the slow τ with an increase in (−) Bay K 8644 concentration in two neonatal rat myocytes and one guinea pig ventricular myocyte.

occurrence of overlapping openings of independent channels at the peak P_o in 1 μM (−) Bay K 8644 compares well with the observed probability of 0.036. The ED_{50} value is close to published values from whole-cell and binding data.

Since we used the maximum-likelihood method to estimate open-time τ's and areas, we have only three free parameters to estimate for a biexponential distribution. Unlike nonlinear least-squares curve fitting, the maximum-likelihood method is independent of binning. Each observation contributes equally to the likelihood product. The number of bins at long times in Fig. 6 does not reflect the number of events used to estimate the τ's and areas. The total number of events, the area of the

slow component, and the number of events in the slow component at 10, 100, and 1,000 nM (−) Bay K 8644 are: 106 total events, 0.33, 35 events; 62 total events, 0.44, 27 events; 108 total events, 0.66, 71 events; respectively. 10 simulations of the data at 10 nM (−) Bay K 8644 with the same number of events and parameter values were constructed. We compared the standard deviation calculated directly from the 10 values of the maximum-likelihood estimates of the slow τ with the mean of the 10 standard deviation estimates produced by the maximum-likelihood routine for each slow τ. The standard deviation of the τ values was 2.05 ms and the mean of the standard deviation estimates was 2.21 ms. Allowing that this is sufficient justification for using the standard deviation estimate at each concentration, the slow τ value at 100 nM (−) Bay K 8644 is not statistically different from the values at either 10 or 1,000 nM. However, the values at 10 and 1,000 are significantly different from each other at greater than the 95% confidence interval.

We expressed the data in Fig. 6 as cumulative open-time distributions and used the Kolmogorov-Smirnov two sample test (Gibbons, 1985), a nonparametric statistic, to determine if the empirical cumulative open-time distributions were significantly different. The empirical distributions are different at greater than the 95% confidence level between 10 and 100 nM and at greater than the 99% confidence level between 100 nM and 1 μM (−) Bay K 8644. Although we can not rigorously establish parameter values of the dose-response relationship of the slow open-time τ from the data in Fig. 6, the observation of clearly distinct nonidentical open-time distributions at different concentrations of DHP agonist is counter to the mechanism proposed for DHP gating of the calcium channel in the mode hypothesis. Values of the fast τ also displayed a concentration-dependent increase in this cell.

A cell-attached patch on an adult guinea pig ventricular myocyte showed an approximately twofold increase in the slow open time τ for an increase in concentration of (+)-S-202-791 stereoisomer from 100 to 500 nM. Hess et al. (1984) concluded that open-time τ's were concentration independent from comparisons of open time τ's at 1 and 0.1 μM racemic Bay K 8644. From our data, the best estimate of (−) Bay K 8644 ED_{50} for the slow open-time τ is small enough to make comparison of τ's at 1 and 0.1 μM unlikely to reveal a concentration dependence since these concentrations are near the saturation range of the binding curve. We have data from a third of three cells examined in this way in which a concentration-dependent increase of open time was present. In one cell a ratio of 12 for the slow τ at 10 nM (−) Bay K 8644 to the τ at 1 nM was found. Kokubun and Reuter (1984) previously reported concentration-dependent slow open-time τ's in neonatal rat cardiac myocytes.

If mode 1 kinetics are unchanged in the presence of DHPs, as the mode model predicts (Fox et al., 1986), cell 3 in Table I would have 96% of its openings in a trace arising from mode 2 activity, but we have not observed mode 2 activity >73% as indicated by the area of the slow component in maximum-likelihood estimates of open-time distribution parameters (area estimate of the slow τ for cell 3 at 1 μM (−) Bay K 8644 is 56%). We observed in five cells an increase in the number of openings per trace in the presence of (−) Bay K 8644 that was greater than the increase of openings due to activity of the DHP-dependent long-lived open state. We conclude that openings of the short-lived open state (mode 1) must be more frequent in the

presence of (−) Bay K 8644. The short-lived open state in the presence of (−) Bay K 8644 can show a decrease in waiting time, (see below), an increase in open time, and an increase in rate of inactivation of summed currents relative to the drug-free short-lived open state. The decreased waiting time and increased decay can be seen in the low P_o summed current (compare with control current) in Fig. 4 *b* of Hess et al. (1984).

One neonatal ventricular myocyte displayed relatively fixed long open-time τ's

TABLE I

DHP Effects on Bursts and Openings per Trace

Parameter	Cell	Control	10^{-9}	10^{-8}	10^{-7}	10^{-6}	SPC*	mV
Openings per trace‡	1§	3.79	4.93	9.33			Neo	10
	3§	0.13		0.73	1.90	3.51	Neo	0
	4§	2.29			5.00		Neo	0
	6§			1.10	1.03	1.66	Neo	20
	6§			0.04	0.23	1.08	Neo	0
	10‖	2.22			15.73	15.46¶	GP	0
Slow open-time τ	1§	0.53‡	1.09‡	1.85‡			Neo	10
	6§			4.21	12.81	21.84	Neo	20
	10‖				4.04	8.99¶	GP	0
Openings per burst	1§	1.42	1.40	1.61			Neo	10
	3§			1.20	1.24	1.34	Neo	0
	4§	1.25			1.71		Neo	0
	6§			2.07	1.46	1.59	Neo	20
	6§					1.36	Neo	0
	10‖	1.48			2.15	2.14¶	GP	0
Total open time in burst (slow τ)	1§	0.88‡	1.52‡	2.97‡			Neo	10
	6§			13.76	20.86	33.38	Neo	20
	10‖	0.73**			6.70	10.89¶	GP	0
Total closed time in burst	1§	2.59	2.35	1.91			Neo	10
	3§			1.16	0.83	0.73	Neo	0
	4§	1.31			1.08		Neo	0
	6§			0.54	1.17	0.87	Neo	20
	10‖	4.98‡			3.04	1.83¶	GP	0

*SPC, species; Neo, neonatal rat; GP, adult guinea pig.
‡Mean value.
§(−) Bay K 8644.
‖(+)-202-791.
¶500 nM DHP.
**Fit by a single exponential.

with an increasing (−) Bay K 8644 concentration (cell 3 in Table I). This cell is distinguished from cells showing concentration-dependent transition rates by having prolonged openings in control conditions. As described above, this cell does show drug-dependent changes in the short-lived open-state kinetics. In this cell we observed an increase in the number of openings per trace, a dose-dependent increase in summed single-channel currents, and a decrease in the latency to first opening.

Brown et al. (1984*a*) using cultured neonatal rat ventricular myocytes found a large increase in P_o but did not observe a significant fraction of prolonged openings and a reduction in waiting time with submicromolar concentrations of DHP agonists as described here. One explanation for this discrepancy is due to the presence of low threshold Ca^{2+} channels in neonatal rat myocytes (Lacerda and Brown, 1986). Ca^{2+} was used as the charge carrier in Brown et al. (1984*a*). Since Ca^{2+} reduces the difference in unitary current amplitudes of high and low threshold channels relative to their values in Ba^{2+} (Carbone and Lux, 1984) their presence in multichannel patches may have been unrecognized. Assuming that 40 mM Ca^{2+} produces approximately the same shift in Ca^{2+} channel gating as 95 mM Ba^{2+} (Wilson et al., 1983; Kass and Krafte, 1987) the holding and test potentials used in Brown et al. (1984*a*) are compatible with activation of low threshold channels in control and DHP treated patches. The combination of persistent low threshold channel activity with weak activation and briefer open times of high threshold channels at the pulse potentials used would obscure the effects of low doses of agonist. In particular, for pulses not far above activation for the high threshold channels, the activation shift of high threshold channels in going from low to high doses of DHP calcium channel agonists would give the appearance of an artificially abrupt transition in Ca^{2+} channel gating and permeation characteristics.

Bursts. We defined bursts according to the criteria described by Colquhoun and Sakmann (1985). To determine the maximum closed time in a burst we used maximum-likelihood estimates of the fast and slow closed-time distribution τ's. Closed times greater than the maximum value were assumed to terminate a burst, while smaller values were assumed to be closed times within a burst. Since this method produces proportionate errors in classifying closed times, the number of channels in a patch will not systematically bias estimates of burst parameters, but will reduce the precision of parameter estimates. (−) Bay K 8644 alters the bursting activity of calcium channels (Table I). Its major effects are on burst duration, open time in a burst, and burst closed times. Burst duration, open times, and total open time were biexponentially distributed while burst closed times and total closed time were monoexponentially distributed. Previously Kokubun and Reuter (1984) described an increase in the number of openings in a burst with racemic Bay K 8644 in cultured neonatal rat ventricular myocytes. We also observed this, cells 4 and 10 in Table I showed 37 and 45% increases in the number of openings in a burst in the presence of 100 and 500 nM DHP, respectively. Total closed times during a burst show concentration-dependent decreases in magnitude (Table I). The long τ from the closed-time histograms (gaps between bursts) also shows a steady decline with concentration (data not shown). At high concentrations unresolved closings can artifactually increase open times. We estimate a system dead time of 0.2 ms for detection of opening or closing transitions with the half amplitude criteria (Colquhoun and Sigworth, 1983). Burst duration increased with concentration except for cell 3 (Table I).

The mode hypothesis predicts transitions within a mode to be much faster than transitions between modes. Under our experimental conditions bursts should occur within one of the modes and bursts with transitions between modes should be rare. We tested this prediction by selecting bursts with a minimum of two openings from

cell 4 in the presence of 100 nM (−) Bay K 8644. Of these bursts with two or more openings, we required that at least one be of 4.2-ms duration or greater. The minimum open time of 4.2 ms is greater than sixfold the fast open-time τ. Hence these bursts have at least one opening arising from the long-lived open state. Since our selection criteria require one opening to have a duration of 4.2 ms or greater in a qualifying burst its pdf would be truncated on the left at 4.2 ms. Therefore we discarded this opening from the data set. When two or more openings were greater than or equal to 4.2 ms the first opening was discarded. Thus all accepted openings are assumed to arise from pdfs with truncation determined only by the resolution of

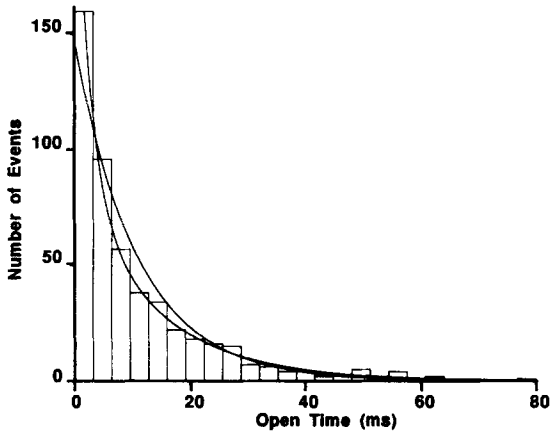

FIGURE 7. Open-time distribution of bursts with at least one long-lived opening. Histogram of the open-time distribution for bursts from a neonatal ventricular myocyte (cell 4) in 100 nM (−) Bay K 8644 with two or more openings of which at least one is of 4.2 ms or a greater duration. Cell-attached recording with 100 mM $BaCl_2$ in the pipette and 140 K-aspartate depolarizing solution in the bath. The cell was held at −40 mV and stepped to 0 mV at a rate of 1 Hz. The first opening of 4.2 ms or greater within an accepted burst is omitted from the distribution. The maximum-likelihood procedure was applied with one exponential probability density function (pdf) and the sum of two exponential pdf's. An estimate of 10.84 ms for the τ of the single exponential pdf was obtained. For the biexponential pdf, estimates for the fast and slow τ of 2.57 and 13.92 ms, respectively, were obtained. The area of the fast component was estimated as 0.27. The area of the slow component is 1–0.27 or 0.73. Note that only one and three parameters were estimated for the mono- and biexponential pdf's. The log-likelihood of the monoexponential pdf was −1,224 and of the biexponential −1,217. This difference in the values of the log-likelihood indicate significantly better parameter estimates with two exponentials at the 99% confidence level. The biexponential pdf is the line with the larger curvature. Data were analog filtered at 3 kHz (−3 dB) with an 8-pole Bessel filter during acquisition and digitally filtered by a zero-phase filter at 1 kHz during channel detection.

the patch-clamp system. We used the maximum-likelihood ratio test to discard the hypothesis of a monoexponential probability density function (pdf) in favor of a biexponential pdf for this data at the 99% confidence level. Since modes are long lived we expect bursts occurring while a channel is in mode 2 to have a monoexponential distribution with a τ value corresponding to the long-lived open state. Within a burst, transitions between modes should be rare since the modes are thought to have a τ in the second range (Hess et al., 1984). The presence of a fast τ in bursts that we attribute to channel activity while in mode 2 indicates an excess of brief

openings due to switching between modes 1 and 2 on a millisecond time scale. This result is incompatible with the presumed long lives of the modes in the mode hypothesis and makes the certain identification of mode behavior much more difficult than envisioned. Maximum-likelihood parameter estimates for open times within qualifying bursts from cell 4 are shown in Fig. 7.

Waiting times. Waiting times are decreased by (−) Bay K 8644 (Hess et al., 1984). Cardiac calcium channels have at least two closed states preceding the open

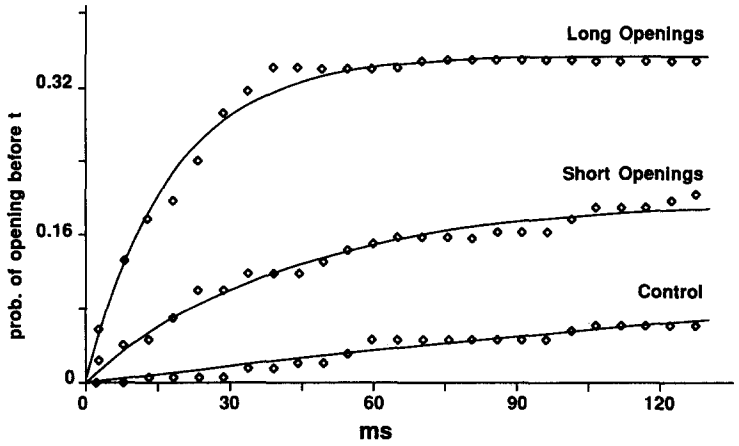

FIGURE 8. Cumulative waiting-time distributions for long and short openings. Cumulative waiting-time distributions in 1 μM (−) Bay K 8644 and in control from a cell-attached patch on a neonatal rat ventricular myocyte with 140 mM K-aspartate depolarizing solution in the bath and 100 mM $BaCl_2$ solution in the pipette. The first opening of each record in 1 μM DHP is sorted into long and short opening sets of data based on its open time by assigning all openings longer than four times the fast open-time distribution τ to the long opening set of data. Fast and slow open-time τ's were 0.64 and 13.99 ms, respectively. Relative areas from maximum-likelihood fits of the open-time distributions were 0.44 and 0.56 for fast and slow components, respectively, and the total number of openings was 316. The waiting-time distributions have been corrected for two channels in the patch and include nulls. Nulls for the sorted sets of data were defined as null records and records with a first opening that did not meet the selection criteria. Control open-time distribution data were not sorted by open time. The waiting-time distribution for long openings, short openings, and control were fit by nonlinear least squares with single τ's of 18 ms (52 openings), 44 ms (33 openings), and 666 ms (12 openings), respectively. Control data were obtained from 100 records, 1 μM (−) Bay K 8644 data were from 90 records. Records were analog filtered by an 8-pole Bessel filter at 3 kHz (−3 dB) and during channel detection by a zero-phase 4-pole filter at 1 kHz. In another neonatal ventricular myocyte analyzed in this way we obtained similar results.

state (Brown et al., 1982; Fenwick et al., 1982; Cavalié et al., 1983) and should show at least a biexponential waiting-time distribution. This is not seen in our control data at room temperature, which is most likely due to the small number of events observed. At elevated temperatures and/or in the presence of (−) Bay K 8644 a biexponential distribution is easily seen. At elevated temperatures resolution of two exponentials is due to an increase in P_o (data not shown). The appearance of the

biexponential distribution at room temperature in the presence of (−) Bay K 8644 is associated with the longer open times and shorter latencies of the drug-dependent long-lived open state. Openings in control or openings of the short-lived open state in the presence of (−) Bay K 8644 have longer latencies relative to the long-lived open state (four cells). As Fig. 8 demonstrates, transitions from closed states to the short- and long-lived open state are different in the presence of (−) Bay K 8644. We examined the significance of the differences in the waiting-time distributions with the Kolmogorov-Smirnov two sample test. The original, uncorrected empirical first latency distributions were significantly different at better than the 97.5% confidence limit between control and brief openings, and at the 99% confidence limit between brief and prolonged openings. The first latency distributions of both the short- and long-lived events can show a dose-dependent decrease in waiting time (cell 6, data not shown). Hoshi and Smith (1987) performed a similar analysis of Ca^{2+} channel first latencies in the presence of Bay K 8644 and found a significantly shorter latency of prolonged openings relative to brief openings.

Closed times. The closed-time frequency distributions show at least two τ's (Brown et al., 1982; Fenwick et al., 1982; Cavalié et al., 1983, 1986; Hess et al., 1984), a fast τ from the gaps within bursts and a slower τ from the gaps between bursts. The fact that we rarely had patches with only a single calcium channel made interpretation of the slow τ difficult. (−) Bay K 8644 appears to decrease both the fast and slow closed times in a dose-dependent manner.

Conductance. The conductance of calcium channels appears to be increased by (−) Bay K 8644 in most neonatal ventricular myocytes we analyzed. Fig. 9 shows a neonatal myocyte maintained at room temperature and stepped to 0 mV from a holding potential of −40 mV at 1 Hz. The amplitude histogram is fitted with the sum of three Gaussian distributions in the presence of 100 nM (−) Bay K 8644. Low threshold Ca^{2+} channels (Carbone and Lux, 1984; Bean, 1985; Nilius et al., 1985; Nowycky et al., 1985*b*) are found in neonatal myocytes (Lacerda and Brown, 1986). We believe the small amplitude component seen in Fig. 9 is not the low threshold calcium channel, which would have a similar amplitude, in part because transitions from the larger amplitudes to the smaller amplitude and back can be seen in the absence of detectable closing to the zero-current level. Moreover, the cell was held at −40 mV, the openings occurred late in the trace, and they were dispersed in time. Low threshold channels are fully inactivated at −40 mV holding potentials in whole-cell measurements and openings are clustered at the onset of the pulse. Five neonatal myocytes showed an increase in conductance in the presence of DHP.

Attenuation of the amplitude of normal, brief openings, by the limited bandwidth of the patch clamp could be misleading, but several aspects of the data suggest that a conductance increase may indeed be an effect of Bay K 8644 on neonatal rat cardiac calcium channels. We have estimated the number of unresolved simultaneous openings and closings of independent channels that could reproduce our observations of multiple conductances in single openings. Using the binomial expression for the probability of all overlapping transitions expected with a 300-μs dead time, we expected to see four overlaps and we identified 28 potential simultaneous transitions with an N of three channels estimated from the maximum observed overlap of unitary currents. The assumption of independence for the

channels is supported by the fair agreement of the estimate of expected overlaps (99) of two channels with the observed overlaps (124) for a three-channel patch with an opening probability per channel of 0.155 determined from the ratio of mean current to the weighted average of unitary current amplitudes.

Most of our amplitude distributions in neonatal and guinea pig myocytes in the presence of DHP agonists are fit by at least two Gaussian components. In eight cells evaluated by the maximum-likelihood ratio criterion for goodness of fit at the 95%

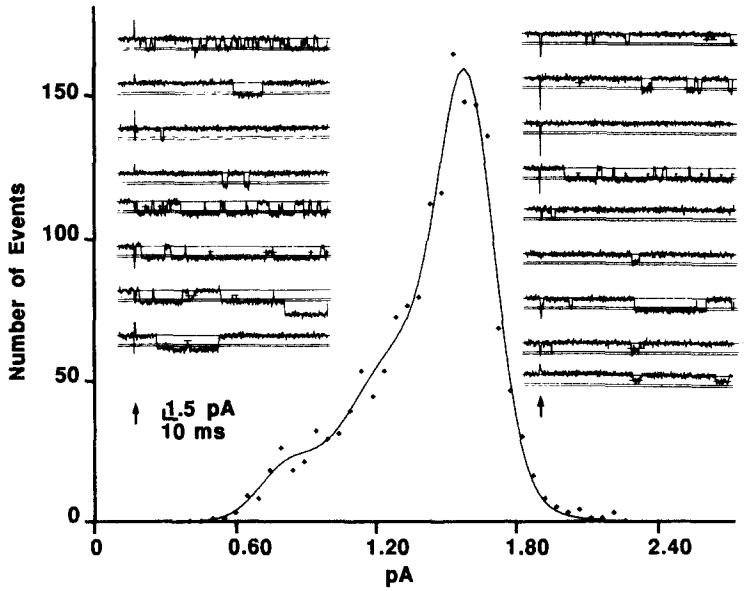

FIGURE 9. Multiple conductance levels in the presence of DHP. Amplitude histogram at 0 mV from a cell-attached patch on a neonatal ventricular myocyte obtained in the presence of 100 nM (−) Bay K 8644 at room temperature with 140 mM K-aspartate depolarizing solution in the bath and 100 mM $BaCl_2$ solution in the pipette. The data were fitted with the sum of three Gaussian distributions by nonlinear least-squares criteria with means (μ), standard deviations (σ), and normalized areas (A) of $\mu_1 = 0.81$, $\sigma_1 = 0.12$, $A_1 = 0.052$; $\mu_2 = 1.34$, $\sigma_2 = 0.25$, $A_2 = 0.503$; $\mu_3 = 1.59$, $\sigma_3 = 0.11$, $A_3 = 0.445$. Single-channel records have lines drawn through the zero-current level and the mean amplitudes obtained from the fits to the data. Arrows indicate the onset of the pulse. Records are not consecutive and are shown filtered at 1 kHz by a 4-pole zero-phase digital filter. Records were analog filtered by an 8-pole Bessel filter at 3 kHz (−3 dB) during acquisition. We observed a conductance increase on exposure to DHP in five neonatal ventricular myocytes.

confidence level only two cells, one in control and the other in 10 nM (−) Bay K 8644, did not show a statistically significant improvement of fit when the number of fitted Gaussians was increased from one to two. Both cells were significantly better fit by multiple Gaussians at higher DHP concentrations. None of the cells examined could be fit by a single Gaussian at micromolar DHP concentrations. Three cells were significantly better fit by four Gaussians, although not at all concentrations of DHP. In Fig. 10 *A* control histogram values are shown superimposed on the fit to

the values in the presence of 100 nM (−) Bay K 8644 (same cell as in Fig. 9). Essentially no openings occur in control data at the largest amplitude level in drug. The open-time τ for this patch was 0.65 ms. Filtering at 1 kHz will not produce such a pronounced reduction in amplitude nor skewing of the distribution if the large amplitude component occurred with any frequency in the control data. Furthermore, our method of channel amplitude determination uses a higher bandwidth than the channel detection algorithm. For this and most cells, amplitudes were

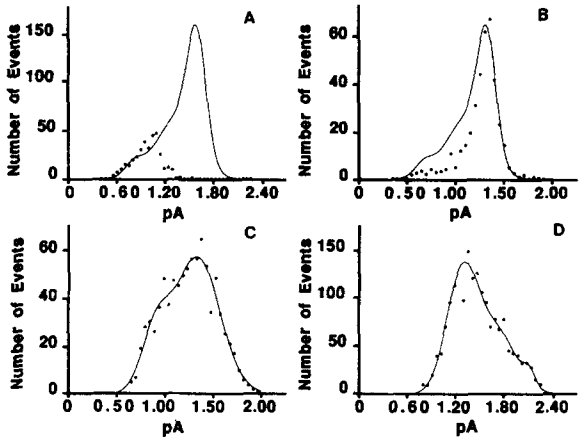

FIGURE 10. Amplitude histograms in control and in the presence of DHP. In *A* control amplitude histogram values from the neonatal ventricular myocyte in Fig. 9 are shown superimposed on the fit to the amplitude histogram in 100 nM (−) Bay K 8644; parameter values for the fit are listed in the legend of Fig. 9. Control data are fitted with the sum of two Gaussian distributions (fit not shown) by nonlinear least-squares criteria with means (μ), standard deviations (σ), and normalized areas (A) of $\mu_1 = 0.74$, $\sigma_1 = 0.11$, $A_1 = 0.231$; $\mu_2 = 1.03$, $\sigma_2 = 0.12$, $A_2 = 0.769$. In *B* amplitude histogram values for opening events in 100 nM (−) Bay K 8644 with durations >2.6 ms are shown superimposed with the fit to all openings at this drug concentration. *C* shows the amplitude histogram from the cell in Fig. 5 *A* obtained in the absence of DHP at 10 mV, 32°C, and analog filtered at 3 kHz bandwidth (8-pole Bessel, −3 dB). The data are fit with the sum of two Gaussian distributions by nonlinear least-squares criteria with parameter values of $\mu_1 = 0.91$, $\sigma_1 = 0.15$, $A_1 = 0.222$; $\mu_2 = 1.34$, $\sigma_2 = 0.23$, $A_2 = 0.778$. In *D* amplitude histogram values at 0 mV from a guinea pig ventricular myocyte at room temperature in the presence of 500 nM (−) Bay K 8644 at 1-kHz bandwidth (4-pole zero-phase digital filter) are shown. The bath solution was 140 mM K-aspartate and the pipette solution was 100 mM $BaCl_2$. The data are fit with the sum of three Gaussian distributions with parameter values of $\mu_1 = 1.07$, $\sigma_1 = 0.16$, $A_1 = 0.617$; $\mu_2 = 1.43$, $\sigma_2 = 0.19$, $A_2 = 0.353$; $\mu_3 = 1.76$, $\sigma_3 = 0.06$, $A_3 = 0.030$.

determined from data filtered at 3 kHz (−3 dB point), while channels were detected in data filtered at 1 kHz.

The properties of our channel detection scheme have been described in Wilson and Brown (1985). When idealized data were analyzed, the method produced skewing of the amplitude distribution, but skewing was undetectable when noise was added to the idealized data. Fig. 10 *B* shows histogram data sorted by open time from the same patch in the presence of drug. Only openings longer than 2.60 ms (four times the open-time τ in control) are shown. The majority of long-lived openings are due to the large amplitude component, although each component contrib-

utes some long openings. The presence of the small amplitude component in Fig. 10 *B* shows that it is not an artifact due to filtering of brief openings. From the minor change in the distributions of the two low amplitude components in Fig. 10 *A* upon exposure to drug, we believe that the large amplitude component reflects a drug-bound open state that is not produced at the expense of the lower amplitude components. Fig. 10 *C* shows control amplitude histogram data obtained at 3 kHz (−3 dB point) bandwidth from the cell in Fig. 5 *A*. These data are less likely to be affected by skewing and are also better fit by a double Gaussian distribution. Fig. 10 *D* shows an amplitude histogram taken from an adult guinea pig ventricular myocyte in the presence of 500 nM (+)-S-202-791. A small component was not resolved in this cell. Recently Chen and Hess (1988) described a subconductance state of the high threshold Ca^{2+} channel in control data from adult guinea pig ventricular myocytes with an amplitude similar to the small component in our amplitude histograms. They attribute this subconductance state to a novel gating pattern of high threshold Ca^{2+} channels differing from the previously described modes.

DISCUSSION

The Mode Model of High Threshold Calcium Channel Gating

The results predicted by the mode model were not found in our experiments; gating of calcium channels having both normal and prolonged openings were altered by

TABLE II

Outcomes of the Mode Hypothesis

	Predicted	Observed
Changes in tail current τ's	−	+
Changes in apparent open-time τ's	−	+
Changes in burst duration τ's	−	+
Changes in waiting times of brief openings	−	+
Correlation among long openings	+	−

(−) Prediction of either no change or no correlation.

DHPs, and the effects on waiting time and closed times were concentration dependent. The model as originally presented (Hess et al., 1984) was supported primarily by the DHP agonist effects with the rest of the support coming from the greater than predicted occurrence of prolonged openings in control. The latter result is disputed by Cavalié et al. (1986) and by the present results. Furthermore, Table II shows the mode model to be contradicted in each of five tests applied to it although the apparent concentration dependence of open times is probably due to bandwidth limits and a concentration-dependent fast closed time. The mode hypothesis also predicts that all DHPs should have the same effects on open times. This is clearly not the case for nitrendipine and Bay K 8644 in the data of Hess et al. (1984). Are there changes that could make the mode model acceptable? At a minimum, DHPs would be required to produce significant gating changes within modes 1 and 2. Such changes would work but at the expense of eliminating the certain identification of modes. We conclude that calcium channel gating as revealed by the effects of

DHPs does not support the mode hypothesis of channel gating. That does not exclude the possibility that slow changes in channel function might occur as proposed by Hess et al. (1984), but the possibility is not supported by the DHP results.

Other Models of DHP Effects on High Threshold Calcium Channel Gating

Substantial evidence for nitrendipine binding with high affinity to an inactivated state as predicted by a modulated receptor hypothesis was first presented by Bean (1984). Similar observations have been made for numerous other DHPs, e.g., Hamilton et al. (1987). Gurney et al. (1985) have used this model to obtain good fits to whole-cell currents produced by photoinactivation of nifedipine in cultured neonatal rat cardiac myocytes. Such models do not deal with prolonged openings, and the models other than the mode model that address this result, such as those of Sanguinetti et al. (1986) and of Bechem and Schramm (1987), cannot explain the shortened waiting times, the increased frequency of shorter open times, and the increase in the number of openings in a burst as DHP concentration is increased. Moreover, the model of Sanguinetti et al. (1986) does not allow for concentration-dependent changes in burst duration although that of Bechem and Schramm (1987) does. Most importantly, these models do not take into account the occurrence of more than one DHP binding site although there are electrophysiological (Uehara and Hume, 1985; Brown et al., 1986) and binding data (Williams et al., 1985; Kokubun et al., 1986; Lee et al., 1987) that have been interpreted in this way. We favor the idea that cooperative binding of DHPs occurs and produces changes in all the kinetically observable states of the channel and in the channel conductance as well (see below).

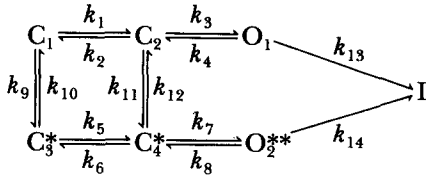

(Scheme 1)

We propose a model in scheme 1 to explain our single-channel results. Closed states C_1 and C_2 bind one DHP molecule in the transitions to C_3^* and C_4^*; C_4^* binds an additional DHP molecule in the transition to the open state O_2^{**}. The second DHP molecule is bound with higher affinity than the first molecule. The magnitude of the concentration-dependent forward rate constant k_7 can be greater than its value in aqueous diffusion if the site is in the membrane and the DHP molecule is restricted to diffusion in two dimensions to access this site (Rhodes et al., 1985), conditions that have been proposed for the binding of DHPs to Ca^{2+} channels. Transition rates are first order except for k_9, k_{11}, and k_7. Normal gating of the Ca^{2+} channel is simulated with rate constants k_1, k_2, k_3, and k_4 with values of 5, 300, 400, and 2,000 s^{-1}. Gating in the presence of agonist DHPs is modeled with k_9, k_{11} equal to 2×10^7 $M^{-1}s^{-1}$ and k_{10}, k_{12} equal to 1 s^{-1}. k_7 is 8×10^{10} $M^{-1}s^{-1}$ and k_5, k_6, and k_8

are 30, 70, and 250 s^{-1}, respectively. Transition rates k_{13} and k_{14} have values of 3 and 30 s^{-1}, respectively, and provide access to an absorbing inactivated state, I. The low affinity K_D is 50 nM and the high affinity K_D is 3 nM.

Simulations of whole-cell peak currents and single-channel open-time data based on this model are shown in Fig. 11. The simulated single-channel open-time data were filtered at 1 kHz to produce a resolution of ~0.2 ms. The latency to first opening of both open states, the closed times, duration of bursts, and number of openings within bursts of the drug-bound open state are concentration dependent. Open

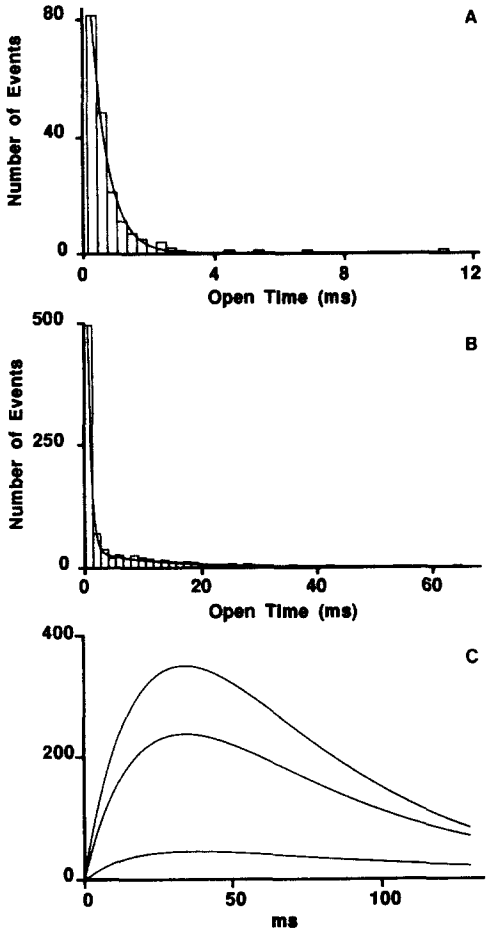

FIGURE 11. Whole-cell and single-channel current simulations. Single-channel current data were simulated by a Monte Carlo technique based on the description in Cox and Miller (1965). Whole-cell currents were simulated by the methods described in Colquhoun and Hawkes (1977). Simulated current records were filtered at 1 kHz with a 4-pole zero-phase digital filter and analyzed in the same manner as data from patch experiments. Scheme 1, with rate constants and values described in the text for 10 and 100 nM DHP, produced the biexponential open-time distributions shown in *A* and *B*. *A* shows simulated data at 10 nM DHP and *B* at 100 nM DHP. In *A* the log-likelihood was significantly improved (> 95%) when a biexponential distribution was used for parameter estimation. The maximum-likelihood estimates of the areas of the fast and slow components were 0.97 and 0.03, respectively, with τ_f = 0.51 and τ_s = 5.46 ms. In *B* at 100 nM DHP the amplitude and τ of the first component was 0.64 and 0.54 ms, respectively, and for slow components it was 0.36 and 11.60 ms, respectively. *C* shows the simulated whole-cell peak current relaxations produced by scheme 1 in dimensionless units for amplitude and time in milliseconds. Inward currents are plotted as positive values. Simulations with 10, 100, and 1,000 nM DHP agonist produce increasingly larger peak currents. Values used for the first-order rate constants of scheme 1 are listed in the text. Second-order rate constants are (in $M^{-1}s^{-1}$) $k_9 = k_{11} = 2 \times 10^7$ and $k_7 = 8 \times 10^{10}$. Values used in the model for these were in 10 nM DHP (in s^{-1}) $k_9 = k_{11} = 0.2$, and $k_7 = 800$; in 100 nM, $k_9 = k_{11} = 2$, and $k_7 = 8{,}000$; in 1,000 nM, $k_9 = k_{11} = 20$, and $k_7 = 80{,}000$.

times are apparently concentration dependent because of the system dead time and the concentration dependence of k_7. For a system dead time of 0.2 ms the probability that a closed time in a burst of $C_4^* - O_2^{**}$ transitions is undetected can be calculated as the probability of a closed time being less than or equal to 0.2 ms for each value of k_7. At 10, 100, and 1,000 nM the calculated probability of an undetected closing is 0.15, 0.80, and 1.00, respectively. This results in apparent concentration dependence of open times (Fig. 11, *A* and *B*). The maximums for observed open times and burst durations of the DHP-bound open state are limited by k_{14} to mean values of 33 ms. Hence open times become concentration independent at saturating doses, as described by Hess et al., (1984). Peak current simulations (Fig. 11 *C*) show three effects we and others observe experimentally (Fig. 1): an increase in peak current and decay rate of current during a step (Sanguinetti et al., 1986), and additionally a reduction in the time to peak (Hess et al. 1984; Markwardt and Nilius, 1988).

Bursts due to the DHP-bound open state can be terminated by initiating a burst of normal openings; the converse is also true. Less often, a burst of O_2^{**} openings may be interrupted by a burst of normal openings, which itself is terminated by initiating a second burst of O_2^{**} openings. We model O_2^{**} as having a larger conductance than O_1 to agree with our observations (Fig. 9). This can reproduce the crenelated appearance we observe rarely in long openings. Furthermore, we expect a fraction of bursts of long openings to be preceded or followed by a burst of normal openings that are not distinguished by the critical close time (t_c) criterion as separate from the burst of long openings. This would give rise to an excess of brief openings in bursts of long openings, in agreement with out data (Fig. 7). The path $C_1 - C_3 - C_4 - C_2$ provides a concentration-dependent means of decreasing the latency (Fig. 8) and increasing P_o of normal openings, as seen in our data.

We have not modeled the voltage-dependent antagonist effects of agonist stereoisomers (Kokubun et al., 1986; Kamp et al., 1987; Kass, 1987). The addition of transitions from closed states to I would account for the <1 limiting probability value of cumulative first latency distributions. We use an absorbing inactivated state here, but a long-lived closed state as described by Cavalié et al. (1986) can replace the inactivated state and allow for steady-state Ca^{2+} channel openings at depolarized potentials (unpublished observations). High affinity of Bay K 8644 for the open state has been suggested previously (McCarthy and Cohen, 1986; Bechem and Schramm, 1987; Beech et al., 1987).

The model proposed in scheme 1 can produce concentration-dependent slow deactivation tail τ's with appropraite transition rates. However, it cannot reproduce the concentration dependence of the fast tail τ. The model in scheme 2 does produce fast and slow concentration-dependent tail τ's and is shown below with transition rates used to model deactivation tail currents.

Scheme 2 differs from scheme 1 by the addition of a third open state with low affinity for DHP agonists, an $O_2^{**} - C_3^*$ transition, and the absence of an inactivated state. Three open states in the presence of DHP agonists is justified by our observation of three Gaussian peaks in our amplitude histogram data. Ma and Coronado (1988) and Yatani et al. (1988) also distinguish by amplitude three open states of the high threshold Ca^{2+} channel in skeletal muscle. An inactivated state was not neces-

sary to model deactivation tail τ's. Addition of transitions from the open states to an inactivated state as in scheme 1 would allow modeling of activation. For simulating deactivation tail currents, C_1 and C_3^* were made absorbing. The low affinity DHP-dependent open state (O_3^*) is modeled as a hydrophilic DHP binding site (Uehara and Hume, 1985) with on rate of 6×10^8 $M^{-1}s^{-1}$. The greater potency of Ba^{2+} relative to Ca^{2+} in reversing DHP antagonist action (Lee and Tsien, 1983) is not due to an effect on membrane surface potential (Kass and Krafte, 1987) and provides support for the existence of a hydrophilic path to a DHP binding site. We fit the concentration dependence of simulated fast and slow deactivation tail τ's with ED_{50}'s of 1 μM and 72 nM, respectively (data not shown). Since none of the transition rates in scheme 2 are obtained from single-channel measurements and the relationship of macroscopic relaxation τ's to microscopic transition rates is complex, we place less weight on the details of scheme 2.

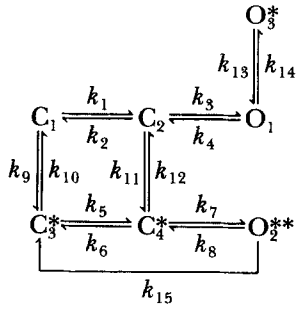

$k_1 = 0\ s^{-1}$
$k_2 = 1{,}800\ s^{-1}$
$k_3 = 200\ s^{-1}$
$k_4 = 4{,}800\ s^{-1}$
$k_5 = 0\ s^{-1}$
$k_6 = 2{,}000\ s^{-1}$
$k_7 = 8 \times 10^{10}\ M^{-1}s^{-1}$
$k_8 = 1{,}600\ s^{-1}$
$k_9 = 0\ s^{-1}$
$k_{10} = 0\ s^{-1}$
$k_{11} = 2 \times 10^7\ M^{-1}s^{-1}$
$k_{12} = 1\ s^{-1}$
$k_{13} = 6 \times 10^8\ M^{-1}s^{-1}$
$k_{14} = 1{,}600\ s^{-1}$
$k_{15} = 600\ s^{-1}$

(Scheme 2)

Tail Currents and Bay K 8644 Effects on Channel Closing

The fast tail τ from macroscopic measurements is dominated by the microscopic closing rate constants from the open states. Extrapolation based on the voltage dependence of the fast tail τ predicts open-time τ values similar to those observed at the higher potentials of the single-channel measurements, taking into account the different divalent ion concentrations. Assuming the fast tail τ can be described as a jump rate over a single energy barrier, the rate constant for this process is an exponential function of barrier height. The exponential term includes both a voltage-dependent and a voltage-independent component. Since Bay K 8644 appears to scale the exponential fast tail τ-V relation with only a small change in slope, the dominant effect of (−) Bay K 8644 must be on the potential-independent free energy term. This term has both enthalpy and entropy components. Our experiments cannot assign the effect of (−) Bay K 8644 to the enthalpy or entropy terms, but experiments varying temperature could determine this. Thermodynamic analy-

sis of DHP binding data show differences in enthalpy and entropy components of binding that depend on the agonist or antagonist nature of the DHP (Mann and Hosey, 1987). By measuring tail τ's at various temperatures, functional correlates to the biochemical data may be observed.

Conductance Increase

One other finding worthy of comment is that the unit conductance was increased by Bay K 8644. There is a correlation with open-time probability density function and at present we have no explanation for its occurrence. Perhaps we are dealing with the response of a different set of calcium channel proteins, although more transitions between conductance levels are observed than are predicted by the assumption of independent channels. However, the fact that conductance is altered in over half of the cases suggests a significant change from normal of the conductive properties of the drug-bound channel.

Previous studies of Brown et al. (1984*a*) and Kokubun and Reuter (1984) described an increase in channel conductance with agonist DHPs. Their data were obtained from cell-attached patches on neonatal rat cardiac myocytes bathed in physiological solutions. Kokubun and Reuter (1984) noted that a change in channel conductance could be due simply to a change in resting potential of the cell caused by the addition of DHP. In our case and for Caffrey et al. (1986) myocytes were depolarized with 140 mM K-aspartate to ~0 mV. Addition of (−) Bay K 8644 under these conditions should have no effect on membrane potential. We interpret the larger conductance channel in our data as a drug-modified channel. It would be informative to observe conductance level changes in these channels in maintained depolarizations.

We thank A. VanDongen for helpful discussion and the use of several analysis routines.

This work was supported by National Institutes of Health grants HL-36930 and HL-37044 to A. M. Brown and HL-07348 to A. E. Lacerda.

Original version received 1 July 1987 and accepted version received 12 December 1988.

REFERENCES

Bean, B. P. 1984. Nitrendipine block of cardiac calcium channels: high-affinity binding to the inactivated state. *Proceedings of the National Academy of Sciences.* 81:6388–6392.

Bean, B. P. 1985. Two kinds of calcium channels in canine atrial cells. Differences in kinetics, selectivity, and pharmacology. *Journal of General Physiology.* 86:1–30.

Bechem, M., M. Kayser, and M. Schramm. 1987. Bay K 8644 modulates the gating of the Ca-channel. *Pflügers Archiv.* 408(Suppl. 1):R39.

Bechem, M., and M. Schramm. 1987. Calcium-agonists. *Journal of Molecular and Cellular Cardiology.* 19(Suppl. II):63–75.

Beech, D. J., T. B. Bolton, and S. Hering. 1987. The mechanism of modulation of Ba^{2+} currents by D600, nitrendipine or Bay K 8644 in single smooth-muscle cells of rabbit ear artery studied using a new concentration jump technique. *Journal of Physiology.* 390:83P.

Bellemann, P. 1984. Binding properties of a novel calcium channel activating DHP in monolayer cultures of beating myocytes. *Federation of European Biochemical Societies Letters.* 167:88–92.

Bellemann, P., and G. Franckowiak. 1985. Different receptor affinities of the enantiomers of Bay K 8644, a dihydropyridine Ca^{2+} channel activator. *European Journal of Pharmacology.* 118:187–188.

Bevington, P. R. 1969. Data Reduction and Error Analysis for the Physical Sciences. McGraw Hill Book Co., New York. 336 pp.

Brown, A. M., H. Camerer, D. L. Kunze, and H. D. Lux. 1982. Similarity of unitary Ca^{2+} currents in three different species. *Nature.* 299:156–158.

Brown, A. M., D. L. Kunze, and A. Yatani. 1984*a*. The agonist effect of dihydropyridines on Ca^{2+} channels. *Nature.* 311:570–572.

Brown, A. M., Y. Tsuda, and D. L. Wilson. 1984*b*. A description of activation and conduction in calcium channels based on tail and turn-on current measurements in the snail. *Journal of Physiology.* 344:549–583.

Brown, A. M., D. L. Kunze, and A. Yatani. 1986. Dual effects of dihydropyridines on whole-cell and unitary calcium currents in single ventricular cells of guinea-pig. *Journal of Physiology.* 379:495–514.

Caffrey, J. M., I. R. Josephson, and A. M. Brown. 1986. Calcium channels of amphibian stomach and mammalian aorta smooth muscle cells. *Biophysical Journal.* 49:1237–1242.

Carbone, E., and H. D. Lux. 1984. A low voltage-activated, fully inactivating Ca^{2+} channel in vertebrate sensory neurons. *Nature.* 310:501–502.

Cavalié, A., R. Ochi, D. Pelzer, and W. Trautwein. 1983. Elementary currents through Ca^{2+} channels in guinea pig myocytes. *Pflügers Archiv.* 398:284–297.

Cavalié, A., D. Pelzer, and W. Trautwein. 1986. Fast and slow gating behavior of single calcium channels in cardiac cells. Relation to activation and inactivation of calcium-channel current. *Pflügers Archiv.* 406:241–258.

Chad, J. E., and R. Eckert. 1986. An enzymatic mechanism for calcium current inactivation in dialyzed *Helix* neurons. *Journal of Physiology.* 378:31–51.

Chen, C., and P. Hess. 1988. A complex new gating pattern detected in L-type calcium channels from guinea-pig ventricular myocytes and mouse 3T3 fibroblasts. *Journal of Physiology.* 390:80P.

Cohen, C. J., and R. T. McCarthy. 1987. Nimodipine block of calcium channels in rat anterior pituitary cells. *Journal of Physiology.* 387:195–225.

Colquhoun, D., and A. G. Hawkes. 1977. Relaxation and fluctuations of membrane currents that flow through drug-operated channels. *Proceedings of the Royal Society London, B.* 199:231–262.

Colquhoun, D., and A. G. Hawkes. 1982. On the stochastic properties of bursts of single ion channel openings and clusters of bursts. *Philosophical Transactions of the Royal Society of London.* 300:1–59.

Colquhoun, D., and A. G. Hawkes. 1987. A note on correlations in single ion channel records. *Proceedings of the Royal Society London, B.* 230:15–52.

Colquhoun, D., and B. Sakmann. 1985. Fast events in single-channel currents activated by acetylcholine and its analogues at the frog muscle end-plate. *Journal of Physiology.* 369:501–557.

Colquhoun, D., and F. J. Sigworth. 1983. Fitting and statistical analysis of single channel records. *In* Single-Channel Recording. B. Sakmann and E. Neher, editors. Plenum Press, New York. 191–263.

Cota, G. 1986. Calcium channel currents in pars intermedia cells of the rat pituitary gland. Kinetic properties and washout during intracellular dialysis. *Journal of General Physiology.* 88:83–105.

Cox, D. R., and H. D. Miller. 1965. The Theory of Stochastic Processes. John Wiley and Sons, Inc., New York.

Fenwick, E. M., A. Marty, and E. Neher. 1982. Sodium and calcium channels in bovine chromaffin cells. *Journal of Physiology.* 331:599–635.

Fox, A. P., P. Hess, J. B. Lansman, B. Nilius, M. C. Nowycky, and R. W. Tsien. 1986. Shifts between modes of calcium channel gating as a basis for pharmacological modulation of calcium influx in cardiac, neuronal, and smooth-muscle-derived cells, *In* New Insights into Cell and Membrane Transport Processes G. Poste and S. T. Crooke, editors. Plenum Press, New York. 99–124.

Gibbons, J. D. 1985. Nonparametric Statistical Inference. Marcel Dekker, Inc., New York. 408 pp.

Gurney, A. M., J. M. Nerbonne, and H. A. Lester. 1985. Photoinduced removal of nifedipine reveals mechanisms of calcium antagonist action on single heart cells. *Journal of General Physiology.* 86:353–379.

Hamill, O., A. Marty, E. Neher, B. Sakmann, and F. J. Sigworth. 1981. Improved patch-clamp techniques for high-resolution current recording from cells and cell-free membrane patches. *Pflügers Archiv.* 391:85–100.

Hamilton, S. L., A. Yatani, K. Brush, A. Schwartz, and A. M. Brown. 1987. A comparison between the binding and electrophysiological effects of dihydropyridines on cardiac membranes. *Molecular Pharmacology.* 31:221–231.

Hess, P., J. B. Lansman, and R. W. Tsien. 1984. Different modes of Ca^{2+} channel gating behavior favored by dihydropyridine Ca^{2+} agonists and antagonists. *Nature.* 311:538–544.

Hess, P., J. B. Lansman, and R. W. Tsien. 1985*a*. Mechanism of calcium channel modulation by dihydropyridine agonists and antagonists. *In* Bayer Symposium IX. Cardiovascular Effects of Dihydropyridine-Type Calcium Antagonists and Agonists. A. Fleckenstein, C. Van Breeman, R. Gross, and F. Hoffmeister, editors. Springer-Verlag, New York. 34–55.

Hess, P., J. B. Lansman, and R. W. Tsien. 1985*b*. Mechanism of calcium channel modulation by dihydropyridine agonists and antagonists. *In* Control and Manipulation of Calcium Movement. J. R. Parrat, editor. Raven Press, New York. 189–212.

Hille, B. 1977. Local anesthetics: hydrophilic and hydrophobic pathways for the drug-receptor reaction. *Journal of General Physiology.* 69:497–515.

Hondeghem, L. M., and B. G. Katzung. 1977. Antiarrhythmic agents: the modulated receptor mechanism of action of sodium and calcium channel-blocking drugs. *Annual Review of Pharmacology and Toxicology.* 24:387–423.

Hoshi, T., and S. J. Smith. 1987. Large depolarization induces long openings of voltage-dependent calcium channels in adrenal chromaffin cells. *Journal of Neuroscience.* 7:571–580.

Hume, J. R., and A. Uehara. 1986. "Creep currents" in single frog atrial cells may be generated by electrogenic Na^+/Ca^{2+} exchange. *Journal of General Physiology.* 87:857–884.

Jackson, M. B., B. S. Wong, C. E. Morris, H. Lecar, and C. N. Christian. 1983. Successive openings of the same acetylcholine receptor channel are correlated in open time. *Biophysical Journal.* 42:109–114.

Janis, R. A., D. Rampe, J. G. Sarmiento, and D. J. Triggle. 1984. Specific binding of a Ca^{2+} channel activator Bay K 8644 to membranes from cardiac muscle and brain. *Biochemical and Biophysical Research Communications.* 121:317–323.

Kamp, T. J., R. J. Miller, and M. C. Sanguinetti. 1987. The "agonist" enantiomer of the dihydropyridine (DHP) 202-791 blocks I_{Ca} at depolarized potentials. *Biophysical Journal.* 51:429*a*. (Abstr.)

Kass, R. S. 1987. Voltage-dependent modulation of cardiac calcium channel current by optical isomers of Bay K 8644: implications for channel gating. *Circulation Research.* 61(Suppl. I): I1–I5.

Kass, R. S., and D. S. Krafte. 1987. Negative surface charge density near heart calcium channels. *Journal of General Physiology.* 89:629–644.

Kokubun, S., B. Prod'hom, C. Becker, H. Porzig, and H. Reuter. 1986. Studies on Ca^{2+} channels

in intact cardiac cells: voltage dependent effects and cooperative interactions of dihydropyridine enantiomers. *Molecular Pharmacology.* 30:571–584.

Kokubun, S., and H. Reuter. 1984. Dihydropyridine derivatives prolong the open state of Ca^{2+} channels in cultured cardiac cells. *Proceedings of the National Academy of Sciences.* 81:4824–4827.

Lacerda, A. E., and A. M. Brown. 1986. Atrotoxin increases probability of opening of single calcium channels in cultured neonatal rat ventricular cells. *Biophysical Journal.* 49:174*a*. (Abstr.)

Lee, R. T., T. W. Smith, and J. D. Marsh. 1987. Evidence for distinct calcium channel agonist and antagonist binding sites in intact cultured embryonic chick ventricular cells. *Circulation Research.* 60:683–691.

Lee, K. S., and R. W. Tsien. 1983. Mechanism of calcium channel blockade by verapamil, D600, diltiazem and nitrendipine in single dialyzed heart cells. *Nature.* 302:790–794.

Ma, J., and R. Coronado. 1988. Heterogeneity of conductance states in calcium channels of skeletal muscle. *Biophysical Journal.* 53:387–395.

Mann, A. C., and M. M. Hosey. 1987. Analysis of the properties of binding of calcium channel activators and inhibitors to dihydropyridine receptors in chick heart membranes. *Circulation Research.* 61:379–388.

Mark, G. E., and F. F. Strasser. 1966. Pacemaker activity and mitosis in cultures of newborn rat heart ventricular cells. *Experimental Cell Research.* 44:217–233.

Markwardt, F., and B. Nilius. 1988. Modulation of calcium channel currents in guinea-pig single ventricular heart cells by the dihydropyridine Bay K 8644. *Journal of Physiology.* 399:559–575.

Matteson, D. R., and C. M. Armstrong. 1986. Properties of two types of calcium channels in clonal pituitary cells. *Journal of General Physiology.* 87:161–182.

McCarthy, R. J., and C. J. Cohen. 1986. The enantiomers of Bay K 8644 have different effects on Ca channel gating in rat anterior pituitary cells. *Biophysical Journal* 49:452*a*. (Abstr.)

Nilius, B., P. Hess, J. B. Lansman, and R. W. Tsien. 1985. A novel type of cardiac calcium channel in ventricular cells. *Nature.* 316:443–446.

Nowycky, M. C., A. P. Fox, and R. W. Tsien. 1985*a*. Long-opening mode of gating of neuronal calcium channels and its promotion by the dihydropyridine calcium agonist Bay K 8644. *Proceedings of the National Academy of Sciences.* 82:2178–2182.

Nowycky, M. C., A. P. Fox, and R. W. Tsien. 1985*b*. Three types of neuronal calcium channel with different calcium agonist sensitivity. *Nature.* 316:440–443.

Ochi, R., N. Hino, and Y. Niimi. 1984. Prolongation of calcium channel open time by the dihydropyridine derivative Bay K 8644 in cardiac myocytes. *Proceedings of the Japanese Academy Series B. Physiological and Biological Sciences.* 60:153–156.

Powell, T., D. A. Terrar, and V. W. Twist. 1980. Electrical properties of individual cells isolated from adult rat ventricular myocardium. *Journal of Physiology.* 302:131–153.

Reuter, H., S. Kokubun, and B. Prod'hom. 1986. Properties and modulation of cardiac calcium channels. *Journal of Experimental Biology.* 124:191–201.

Reuter, H. R., H. Porzig, S. Kokubun, and B. Prod'hom. 1985. 1,4-dihydropyridines as tools in the study of Ca^{2+} channels. *Trends in Neurosciences.* 8:396–400.

Reuter, H., C. F. Stevens, R. W. Tsien, and G. Yellen. 1982. Properties of single calcium channels in cardiac cell culture. *Nature.* 297:501–504.

Rhodes, D. G., J. G. Sarmiento, and L. G. Herbette. 1985. Kinetics of binding of membrane-active drugs to receptor sites. *Molecular Pharmacology.* 27:612–623.

Sanguinetti, M. C., D. S. Krafte, and R. S. Kass. 1986. Voltage-dependent modulation of Ca^{2+} channel current in heart cells by Bay K 8644. *Journal of General Physiology.* 88:369–392.

Tsien, R. W., P. Hess, J. B. Lansman, and K. S. Lee. 1985. Current views of cardiac calcium channels and their response to calcium antagonists and agonists. *In* Cardiac Electrophysiology and Arrhythmias. D. P. Zipes and J. Jalife, editors. Grune & Stratton, Inc., Orlando. 19–30.

Uehara, A., and J. R. Hume. 1985. Interactions of organic calcium channel antagonists with calcium channels in single frog atrial cells. *Journal of General Physiology.* 85:621–647.

Williams, J. S., I. L. Grupp, G. Grupp, P. L. Vaghy, L. Dumont, A. Schwartz, A. Yatani, S. Hamilton, and A. M. Brown. 1985. Profile of the oppositely acting enantiomers of the dihydropyridine 202-791 in cardiac preparations: receptor binding, electrophysiological, and pharmacological studies. *Biochemical and Biophysical Research Communications.* 131:13–21.

Wilson, D. L., and A. M. Brown. 1985. Effect of limited interval resolution on single channel measurements with application to Ca^{2+} channels. *IEEE Transactions on Biomedical Engineering.* 32:786–797.

Wilson, D. L., K. Morimoto, Y. Tsuda, and A. M. Brown. 1983. Interaction between calcium ions and surface charge as it relates to calcium currents. *Journal of Membrane Biology.* 72:117–130.

Yatani, A., Y. Imoto, J. Codina, S. L. Hamilton, A. M. Brown, and L. Birnbaumer. 1988. The stimulatory G protein of adenyl cyclase, G_s, also stimulates dihydropyridine-sensitive Ca^{2+} channels. *Journal of Biological Chemistry.* 263:9887–9895.